

## Synthesis and in vitro biodegradation of pure octacalcium phosphate spheres

Journal:	<i>International Journal of Applied Ceramic Technology</i>
Manuscript ID	ACT-5471.R1
Manuscript Type:	Article
Date Submitted by the Author:	n/a
Complete List of Authors:	Tripathi, Garima; Kyushu Kogyo Daigaku - Wakamatsu Campus Miyazaki, Toshiki; Kyushu Kogyo Daigaku - Wakamatsu Campus,
Keywords:	bioceramics, calcium phosphate, particles
Author-supplied Keyword: If there is one additional keyword you would like to include that was not on the list, please add it below::	Biodegradation

SCHOLARONE™  
 Manuscripts

This is the peer reviewed version of the following article: <https://ceramics.onlinelibrary.wiley.com/doi/full/10.1111/ijac.13371>, which has been published in final form at <https://doi.org/10.1111/ijac.13371>. This article may be used for non-commercial purposes in accordance with Wiley Terms and Conditions for Self-Archiving.

1  
2  
3  
4  
5  
6  
7 **Synthesis and *in vitro* biodegradation of pure octacalcium phosphate**  
8  
9 **spheres**  
10  
11  
12  
13  
14  
15

16 **Garima Tripathi and Toshiki Miyazaki**  
17  
18  
19

20  
21 Graduate School of Life Science and Systems Engineering,  
22  
23 Kyushu Institute of Technology, 2-4, Hibikino, Wakamatsu-ku, Kitakyushu 808-0196, Japan  
24  
25

26  
27  
28  
29 Corresponding author:  
30

31  
32 Garima Tripathi and Toshiki Miyazaki  
33

34 Graduate School of Life Science and Systems Engineering, Kyushu Institute of Technology,  
35  
36 2-4, Hibikino, Wakamatsu-ku, Kitakyushu 808-0196, Japan  
37

38  
39 Tel/Fax: +81-93-695-6025  
40

41 E-mail: [garima.msp@gmail.com](mailto:garima.msp@gmail.com)/[tmiya@life.kyutech.ac.jp](mailto:tmiya@life.kyutech.ac.jp)  
42  
43  
44  
45  
46  
47  
48  
49  
50  
51  
52  
53  
54  
55  
56  
57  
58  
59  
60

## Abstract

Octacalcium phosphate (OCP) is a key precursor of biological apatite in hard tissues with excellent osteoconductive and biodegradable properties for bone regeneration. OCP spherical granules are expected to be useful as drug delivery carriers, since OCP has high specific surface area. Although there have been some reports of OCP sphere preparation, methods for preparing pure OCP spheres are limited. The objective of this study is the preparation of spherical granules of pure OCP and assessment of their *in vitro* biodegradation in physiological conditions. We successfully prepared spherical pure OCP granules with a size of  $\sim 500 \mu\text{m}$  without any organic additives by simple immersion of  $\alpha$ -tricalcium phosphate spherical granules in pH 5.0 acetate buffered solutions at  $60^\circ\text{C}$ . The granules had core-shell structure composed of OCP crystals different particle size. The spherical granules showed 20%–40% *in vitro* degradation in physiological conditions, however the phase transition of OCP was not significantly observed.

**Keywords:** Pure OCP sphere,  $\alpha$ -TCP, Acetate buffer treatment, *in vitro* biodegradation

## 1. Introduction

Octacalcium phosphate (OCP:  $\text{Ca}_8(\text{HPO}_4)_2(\text{PO}_4)_4 \cdot 5\text{H}_2\text{O}$ ) has attracted significant interest as a bone substitute because of excellent tissue response. Its osteoconductivity is greatly advanced compared with that of hydroxyapatite (HAp:  $\text{Ca}_{10}(\text{PO}_4)_6(\text{OH})_2$ ), a common bone substitute used in clinical practice. Based on its structural similarity to HAp and its significantly higher solubility and its detection in several calcified tissues, OCP is thought to be involved in the first stages of the tissue biomineralization [1,2]. OCP is a metastable phase of calcium phosphate replaced by new bone through bone remodeling [3,4]. Metastable phases may be fabricated under the following conditions: (1) the solubility of the precursor is higher than that of the metastable phase and (2) the fabrication of the metastable product occurs more rapidly than its transformation to the most stable phase.

OCP is hydrolyzed in aqueous solution and is converted into HAp, while OCP can be obtained by hydrolysis of  $\alpha$ -tricalcium phosphate ( $\alpha$ -TCP:  $\alpha\text{-Ca}_3(\text{PO}_4)_2$ ) [5].  $\alpha$ -TCP can also hydrolyze directly to calcium deficient HAp, depending on the reaction conditions [6]. The interest in the chemical nature of the possible products of  $\alpha$ -TCP hydrolysis, has led to its increasing use in calcium phosphate bioactive bone cements [7,8].

OCP shows excellent biomedical properties and some clinical trial has recently started [9-12]. The present drawback of OCP is difficulty to obtain large single component structures as it easily decomposes under sintering conditions [13-16]. Teshima *et al.* [17] prepared spherical composites of OCP and agarose using a hydrogel method. Murakami *et al.* prepared OCP granules by grinding dried OCP cake using a pestle and mortar [18]. The size of the granules was controlled by sieving, but their shape was not controlled. Recently, Ioku *et al.* [19] reported the preparation of porous OCP spheres using 10 mass % gelatin as a base slurry, followed by sintering. The granules were quite large in size, around 1.0 mm in diameter, and the phase obtained was a mixture of HAp and OCP.

1  
2  
3 In this study, spherical granules of pure OCP were prepared from  $\alpha$ -TCP in the  
4 absence of any supporting polymer or polymeric slurry. Spherical granules are advantageous  
5 from a practical perspective because they can be easily applied at bone-defect sites using a  
6 catheter owing to their fluidity. We therefore aimed to make spheres of OCP that could be  
7 used as a drug delivery system and for bone defect implantation.  
8  
9  
10  
11  
12  
13  
14  
15  
16

## 17 **2. Materials and methods:**

18  
19  $\alpha$ -TCP powder ( $\alpha$ -TCP-B, Taihei Chem. Inc., Osaka, Japan) was used as obtained.  
20 Physiological saline with pH 5.4 was purchased from Otsuka Pharmaceutical Company,  
21 Japan. The other reagents were purchased from Wako Pure Chemical Industries, Ltd., Japan.  
22 Ultrapure water (prepared using a Direct-Q, Nihon Millipore K.K., Tokyo, Japan) was used  
23 for the experiments.  
24  
25  
26  
27  
28  
29  
30  
31  
32

### 33 **2.1 Preparation of $\alpha$ -TCP granules:**

34  
35 The water-in-oil (W/O) emulsion method was used to prepare  $\alpha$ -TCP spherical  
36 granules. An  $\alpha$ -TCP suspension was prepared by adding an equal ratio (weight to volume) of  
37  $\alpha$ -TCP powder to ultrapure water. The suspension was then added dropwise to a 1000-mL  
38 glass beaker containing vegetable oil at 60°C using a pipette. The vegetable oil was stirred  
39 continuously at 500 rpm at 60°C for 2 h to allow the  $\alpha$ -TCP suspension to set into spherical  
40 granules. The granules were then left in the oil to sediment at the bottom. The spherical  
41 granules were collected by filtering the oil followed by washing with acetone to remove  
42 excess oil, and then dried overnight at ambient temperature. The dried spherical granules  
43 were sintered at 1300°C for 3 h and then sieved to obtain  $\alpha$ -TCP spherical granules with a  
44 diameter of ~500  $\mu$ m.  
45  
46  
47  
48  
49  
50  
51  
52  
53  
54  
55  
56  
57  
58  
59  
60

## 2.2 Acetate buffer treatment of $\alpha$ -TCP granules:

The obtained  $\alpha$ -TCP spherical granules (0.10 g) were added to a polypropylene tube containing 20 mL of 0.2 M acetic acid–sodium acetate buffer solution, pH 5.0, at  $60\pm 1.0^\circ\text{C}$ , and the tube was placed in an incubator with continuous shaking for 6 h. Subsequently, the granules were collected, washed with ultrapure water, and dried.

## 2.3 Material characterization:

The surface morphology changes of the samples were characterized using a scanning electron microscope (SEM; S-3500N; Hitachi Co., Tokyo, Japan), an energy dispersive X-ray analyzer (EDX; EX-400; Horiba Co., Kyoto, Japan), an X-ray diffractometer (XRD; MXP3V; Mac Science Ltd., Yokohama, Japan), and a Fourier-transform infrared spectrometer (FT-IR, FT/IR-6100, JASCO Co., Tokyo, Japan). For FT-IR, the samples were ground and mixed with KBr powder at a mass ratio of 1:100 then a thin film was prepared by uniaxially pressing the mixture. For the TEM examinations, the powdered OCP flakes were separated in ethanol solution using ultrasonic vibration, and then picked up with TEM copper grids (STEM Cu 100P (#09-1002), Nisshin EM Co., Ltd., Tokyo, Japan) coated with amorphous carbon film, without a thinning process. The examinations were conducted in the TEM system (TEM, H-9000 NAR, Hitachi Ltd., Tokyo, Japan) with a maximum acceleration voltage of 250 kV.

2.4. The apparent porosity of the prepared OCP spheres were measured according to Archimedes' principle. A porous sample with a dry weight  $W_1$  was filled with water in a beaker *in vacuo*. Measured weight of the water-filled sample in water and air was denoted as  $W_2$  and  $W_3$ , respectively. The apparent porosity can be calculated as follows:

$$\text{Apparent Porosity (\%)} = (W_3 - W_1) / (W_3 - W_2) \times 100 \quad (1)$$

## 2.4 Assessment of *in vitro* biodegradation:

1  
2  
3 The OCP spheres of 500 mg were incubated in 20 mL of phosphate buffered saline  
4 (PBS) or physiological saline at 37°C for various time periods. PBS with ion concentration of  
5  
6 10 mM  $\text{PO}_4^{3-}$ , 137 mM  $\text{Na}^+$ , 2.7 mM  $\text{K}^+$  and pH 7.4 was prepared in the laboratory.  
7  
8  
9

10 OCP degradation was monitored by measuring the dry weight loss over time. At least  
11  
12 four samples at each time point were used to obtain the weight loss curve. Experiments were  
13  
14 carried out under sterile conditions to prevent bacterial and fungal contamination.  
15  
16  
17  
18

### 19 3. Results and Discussion:

20  
21  
22 Figure 1 shows SEM images of the surfaces of the prepared  $\alpha$ -TCP spheres before and  
23  
24 after immersion in acetate buffer solutions for 6 h. The obtained spheres were  $\sim 500$   $\mu\text{m}$  in  
25  
26 diameter. After immersion, the smooth surface morphology was completely converted into  
27  
28 aggregated plate-like particles around 5–10  $\mu\text{m}$  in length.  
29  
30  
31

32  
33 Figure 2 shows SEM images of the pits formed on the  $\alpha$ -TCP spheres after immersion  
34  
35 in acetate buffer solutions for 6 h. Both the top surface and the inside were composed of the  
36  
37 plate-like particles, and that the former is more densely packed and composed of smaller  
38  
39 particles than the latter. It is thought that the dense shell was constructed on the top surface  
40  
41 by rapid reaction of  $\alpha$ -TCP with buffer solution, while its diffusion into the inside of the  
42  
43 granule was suppressed, resulting in slow crystal growth of OCP with larger particle size.  
44  
45  
46

47  
48 Figure 3 shows XRD patterns of  $\alpha$ -TCP spheres after immersion in acetate buffer  
49  
50 solutions for various time periods. Only diffraction peaks attributed to  $\alpha$ -TCP (JCPDS card  
51  
52 9–348) were observed before the immersion. OCP peaks (PDF# 26-1056) appeared after 1 h  
53  
54 and those of  $\alpha$ -TCP were no longer detected after 3 h. Subsequently, the intensity of the OCP  
55  
56 peaks increased. Although many diffraction peaks of the OCP and HAp patterns overlap, a  
57  
58 peak around  $11^\circ$  is only observed for HA, therefore, as no peaks in that position were  
59  
60

1  
2  
3 observed for the sphere immersed for 6 h, it is thought to be composed of pure OCP.  
4  
5 Additionally, calcium hydrogen phosphate dihydrate, which can be formed from  $\alpha$ -TCP in  
6  
7 acidic conditions, was not detected, indicating that  $\alpha$ -TCP was directly hydrolyzed to OCP.  
8  
9

10  
11 **It is noted that pure OCP spheres can be obtained using the present technique with the**  
12  
13 **porosity of  $37\pm 3\%$ .** It has been reported that the coexistence of organic polymers such as  
14  
15 poly-L-glutamate and polyacrylate inhibits the transformation of amorphous calcium  
16  
17 phosphate into HAp [20]; therefore not using organic polymers may enhance the conversion  
18  
19 into OCP. XRD did not reveal significant amounts of other residual phases in the obtained  
20  
21 spheres. The components of  $\alpha$ -TCP are the same as those of OCP:  $\text{Ca}^{2+}$  and  $\text{PO}_4^{3-}$ . Therefore,  
22  
23 incorporation of other ions can be suppressed for this technique, unlike for the technique  
24  
25 using calcium sulfate as a precursor [21]. This method also allows for the production of pure  
26  
27 OCP blocks.  
28  
29  
30  
31

32  
33 Figure 4 shows FT-IR spectra of the synthesized  $\alpha$ -TCP granules before and after  
34  
35 immersion in acetate buffer. No other foreign peaks were detected. After immersion, bands  
36  
37 derived from  $\text{PO}_4^{3-}$  groups ( $560\text{--}600$  and  $1030\text{--}1090\text{ cm}^{-1}$ ) were clearly visible. The  
38  
39 assignment of the absorption peaks of OCP was based on a previous report [22]. In pure  
40  
41 OCP, absorption peaks at  $1193$ ,  $\sim 1120$ ,  $\sim 1034$ ,  $601$ , and  $560\text{ cm}^{-1}$  were assigned to the OH in  
42  
43 plane-bending mode of  $\text{HPO}_4$  in the hydrated layer,  $\text{HPO}_4$  stretching mode,  $\text{PO}_4$  stretching  
44  
45 mode,  $\text{PO}_4$  bending mode, and  $\text{PO}_4$  bending mode, respectively.  
46  
47  
48

49  
50 Figure 5 (a) shows the TEM dark-field image of OCP obtained from  $\alpha$ -TCP. OCP  
51  
52 particles were found to have plate-shaped morphology with smooth edges. Figure 5(b) shows  
53  
54 the electron diffraction pattern of the white circled region in Fig. 5 (a). Similar electron  
55  
56 diffraction patterns were also obtained from other crystallites of OCP. The spots were  
57  
58 assigned to the 110 and 001 planes based on the consideration that these assignments indicate  
59  
60

1  
2  
3 plane spacings of 0.94 and 0.68 nm, respectively; and these are consistent with reported  
4 values,  $d_{110}$  (0.938 nm) and  $d_{001}$  (0.683 nm) [23–24]. Moreover, the line through the 001  
5 and center spots and the line through the 110 and center spots crossed with an angle of  $90.3^\circ$ ,  
6 and this is consistent with the fact that the calculated angle between the (110) and (001)  
7 planes of OCP is  $90.32^\circ$ . The images revealed that the long axis direction of the starting  
8 material of OCP was [001].  
9

10  
11  
12  
13  
14  
15  
16  
17 As a preliminary model of the bioabsorption of the obtained OCP spheres at an  
18 injection site, degradation was monitored *in vitro* by measuring the dry weight of the samples  
19 as a function of incubation time in physiological saline (pH 5.4) and PBS (pH 7.4) (Fig. 6).  
20  
21  
22  
23  
24  
25  
26  
27  
28  
29  
30  
31  
32  
33  
34  
35  
36  
37  
38  
39  
40  
41  
42  
43  
44  
45  
46  
47  
48  
49  
50  
51  
52  
53  
54  
55  
56  
57  
58  
59  
60

Approximately 20% weight loss was observed in the case of physiological saline after up to 21 days. In contrast, the weight loss was around 40% at 21 days of PBS incubation.

Figure 7 shows SEM images of the OCP spheres before and after immersion in saline solution and PBS. Images of the crushed sample are also given to show the morphological changes inside the spheres. The surface morphology of the top surface became smoother as the immersion time increased, while the morphology of the crushed spheres was almost the same. Additionally, the spherical shape was maintained even after 14 days. These results suggest that degradation of the spheres occurs mainly at the surface. The Ca/P molar ratio of pure OCP before immersion was 1.33, while that after immersion in physiological saline and PBS for 14 days was 1.62 and 1.63, respectively. It was also confirmed by XRD that no phase transition of OCP was observed even after soaking in PBS for 21 days (Data not shown). Figure 8 shows a histogram of the particle size distribution of the spheres treated with acetate buffer for 6 h before and after immersion in physiological saline (pH 5.4) and PBS (pH 7.4) solutions at  $37^\circ\text{C}$  for 21 days. The distribution shifted to smaller sizes after immersion, indicating that the spheres are partially dissolved in physiological conditions.

1  
2  
3 Although there are no reports of *in vitro* degradation of OCP, Persson *et al.* [25]  
4 recently reported the long-term *in vitro* degradation of brushite cement in water, PBS, and  
5 serum solution. They observed that specimens in PBS showed the highest degradation rate,  
6 which agrees with the results of our study. However, we observed higher degradation rates,  
7 both in PBS (13.3%/week) and physiological saline solution (6.7%/week), than they reported  
8 (0.22–0.37%/week). Grover *et al.* [26] reported a sharp contrast between the total mass loss  
9 of  $\beta$ -TCP cement aged in bovine serum (57 wt%) compared with that aged in PBS (16 wt%)  
10 over 90 days. The observed degradation was much higher than the theoretical solubility  
11 estimated from the solubility product of OCP ( $pK_{sp} = 48 - 49$ ) [27]. Judging from the result in  
12 Fig. 7 that morphology of the spheres was changed after the immersion, not only chemical  
13 dissolution but also detachment of the constituent particles may occur. In summary,  
14 degradation behavior depends on numerous factors including the porosity, formation of an  
15 outer layer, object volume, phase composition, and degradation media.  
16  
17  
18  
19  
20  
21  
22  
23  
24  
25  
26  
27  
28  
29  
30  
31  
32

33 It can be seen in Figs. 6–7 and from the Ca/P ratio results that the spheres were  
34 partially degraded in physiological conditions, but that phase transition of OCP did not  
35 significantly occur, except at the top surface. Recently, Ban *et al.* [28] also reported that OCP  
36 did not transform to HA in simulated body fluid (SBF) with ion concentrations approximately  
37 equal to those of human blood plasma. Yokoi *et al.* [29] reported that OCP did not transform  
38 to HAp and that further OCP formation occurred on OCP crystals in SBF. Although HAp is a  
39 more stable crystal phase than OCP in SBF, the crystal growth of OCP proceeded differently.  
40 These phenomena were theoretically explained by Liu *et al.* [30]. They conducted a  
41 theoretical analysis of calcium phosphate precipitation in SBF, revealing that the nucleation  
42 rate of OCP is substantially higher than that of HAp, while HAp is thermodynamically more  
43 stable than OCP in SBF. Because of the kinetically slow HAp nucleation, the crystal growth  
44  
45  
46  
47  
48  
49  
50  
51  
52  
53  
54  
55  
56  
57  
58  
59  
60

1  
2  
3 of OCP was thought to occur preferentially. Our results are in accordance with the above  
4 reports.  
5  
6  
7  
8  
9

#### 10 **4. Conclusions:**

11  
12 Spherical pure OCP granules with porosity of 37% were prepared by phase transition  
13 of  $\alpha$ -TCP granules in acidic conditions. Interestingly, they exhibited a kind of core-shell  
14 structure. It is expected that ability of drug delivery can be appropriately controlled by the  
15 thickness of the shell. They showed *in vitro* degradation of 20%–40% in physiological  
16 conditions while maintaining their spherical shape. The spheres have potential uses as  
17 components of bioabsorbable injectable pastes and as pure OCP blocks for bone substitutes.  
18  
19  
20  
21  
22  
23  
24  
25  
26  
27

#### 28 **Conflicts of interest**

29  
30 The authors report no conflicts of interest in this work.  
31  
32  
33  
34

#### 35 **Acknowledgements:**

36  
37 The authors sincerely acknowledge Takeda Science Foundation for designating Dr.  
38 Garima Tripathi a Takeda Fellow and providing the financial support to carry out the  
39 research. We thank Sarah Dodds, PhD, from Edanz Group ([www.edanzediting.com/ac](http://www.edanzediting.com/ac)) for  
40 editing a draft of this manuscript.  
41  
42  
43  
44  
45  
46  
47  
48  
49  
50  
51  
52  
53  
54  
55  
56  
57  
58  
59  
60

**References:**

1. Nelson DGA, Barry JC. High resolution electron microscopy of nonstoichiometric apatite crystals. *Anat Rec.* 1989;224:265-276. [doi.org/10.1002/ar.1092240217](https://doi.org/10.1002/ar.1092240217)
2. Elliott JC. Structure and chemistry of the apatites and other calcium orthophosphates. Elsevier Science; 1994.
3. Kamakura S, Sasano Y, Shimizu T, Hatori K, Suzuki, Kagayama M, Motegi K. Implanted octacalcium phosphate is more resorbable than  $\beta$ -tricalcium phosphate and Hydroxyapatite. *J Biomed Mater Res.* 2002;59:29-34. [doi.org/10.1002/jbm.1213](https://doi.org/10.1002/jbm.1213)
4. Sugiura Y, Onuma K, Kimura Y, Miura H, Tsukamoto K. Morphological evolution of precipitates during transformation of amorphous calcium phosphate into octacalcium phosphate in relation to role of intermediate phase. *J Cryst Growth.* 2011;332:58-67. [doi.org/10.1016/j.jcrysgro.2011.07.030](https://doi.org/10.1016/j.jcrysgro.2011.07.030)
5. Graham S, Brown PW. The low temperature formation of octacalcium phosphate. *J Cryst Growth.* 1993;132:215-225. [doi.org/10.1016/0022-0248\(93\)90265-X](https://doi.org/10.1016/0022-0248(93)90265-X)
6. Durucan C, Brown PW.  $\alpha$ -Tricalcium phosphate hydrolysis to hydroxyapatite at and near physiological temperature. *J Mater Sci Mater Med.* 2000;11:365-371. [doi.org/10.1023/A:1008934024440](https://doi.org/10.1023/A:1008934024440)
7. Fernandez E, Gil FJ, Ginebra MP, Driessens FCM, Planell J, Best SM. Calcium phosphate bone cements for clinical applications. Part II: precipitate formation during setting reactions. *J Mater Sci Mater Med.* 1999;10:177-183. [doi.org/10.1023/A:100898952](https://doi.org/10.1023/A:100898952)
8. Driessens FCM, Boltong MG, De Maeyer EAP, Verbeeck RMH, Wenz R. Effect of temperature and immersion on the setting of some calcium phosphate cements. *J Mater Sci Mater Med.* 2000;11:453-457. [doi.org/10.1023/A:100894412](https://doi.org/10.1023/A:100894412)

- 1  
2  
3 9. Ishiko-Uzuka R, Anada T, Kobayashi K, Kawai T, Tanuma Y, Sasaki K, Suzuki O.  
4  
5 Oriented bone regenerative capacity of octacalcium phosphate/gelatin composites  
6  
7 obtained through two-step crystal preparation method. *J of Biomed Materials Research*  
8  
9 *Part B:App Biomater.* 2017;105:1029-1039. [doi.org/10.1002/jbm.b.33640](https://doi.org/10.1002/jbm.b.33640)  
10  
11
- 12 10. Sai, Y., Shiwaku, Y., Anada, T., Tsuchiya, K., Takahashi, T., Suzuki, O. Capacity of  
13  
14 octacalcium phosphate to promote osteoblastic differentiation toward osteocytes in vitro.  
15  
16 *Acta biomaterialia*, 2018;69:362-371. [doi.org/10.1016/j.actbio.2018.01.026](https://doi.org/10.1016/j.actbio.2018.01.026)  
17  
18
- 19 11. Miura KI, Sumita Y, Kajii F, Tanaka H, Kamakura S, Asahina I. First clinical application  
20  
21 of octacalcium phosphate collagen composite on bone regeneration in maxillary sinus  
22  
23 floor augmentation: A prospective, single-arm, open-label clinical trial. *J of Biomed*  
24  
25 *Materials Research Part B:App Biomater.* 2019 (Published online).  
26  
27 [doi.org/10.1002/jbm.b.34384](https://doi.org/10.1002/jbm.b.34384)  
28  
29
- 30 12. de Souza DC, de Abreu HDLV, de Oliveira PV, Capelo LP, Passos-Bueno MR, Catalani  
31  
32 LH. A fast degrading PLLA composite with a high content of functionalized octacalcium  
33  
34 phosphate mineral phase induces stem cells differentiation. *J Mech Behav Biomed*  
35  
36 *Mater.* 2019;93:93–104. [doi.org/10.1016/j.jmbbm.2019.02.003](https://doi.org/10.1016/j.jmbbm.2019.02.003)  
37  
38
- 39 13. Nelson DGA, McLean JD. High-resolution electron microscopy of octacalcium  
40  
41 phosphate and its hydrolysis products. *Calcified Tissue Int.* 1984;36:219–232.  
42  
43 [doi.org/10.1007/BF02405321](https://doi.org/10.1007/BF02405321)  
44  
45
- 46 14. Ito N, Kamitakahara M, Yoshimura M, Ioku K. Importance of nucleation in  
47  
48 transformation of octacalcium phosphate to hydroxyapatite. *Mater Sci Eng C.*  
49  
50 2014;40:121–126. [doi: 10.1016/j.msec.2014.03.034](https://doi.org/10.1016/j.msec.2014.03.034)  
51  
52
- 53 15. Suzuki O, Nakamura M, Miyasaka Y, Kagayama M, Sakurai M. Bone formation on  
54  
55 synthetic precursors of hydroxyapatite. *Tohoku J Exp Med.* 1991;164:37-50.  
56  
57 [doi.org/10.1620/tjem.164.37](https://doi.org/10.1620/tjem.164.37)  
58  
59  
60

16. LeGeros RZ. Preparation of octacalcium phosphate (OCP): A direct fast method. *Calcif Tissue Int.* 1985;37:194–197. [doi.org/10.1007/BF02554841](https://doi.org/10.1007/BF02554841)
17. Teshima K, Sakurai M, Lee SH, Yubuta K, Ito S, Suzuki T, Shishido T, Endo M, Oishi S. Morphologically Controlled Fibrous Spherulites of an Apatite Precursor Biocrystal. *Crystal Growth & Design.* 2008;9:650-652. [doi.org/10.1021/cg800791s](https://doi.org/10.1021/cg800791s)
18. Murakami Y, Honda Y, Anada T, Shimauchi H, Suzuki O. Comparative study on bone regeneration by synthetic octacalcium phosphate with various granule sizes. *Acta Biomater.* 2010;6:1542-1548. [doi.org/10.1016/j.actbio.2009.10.023](https://doi.org/10.1016/j.actbio.2009.10.023)
19. Ito N, Kamitakahara M, Ioku K. Preparation and evaluation of spherical porous granules of octacalcium phosphate/hydroxyapatite as drug carriers in bone cancer treatment. *Mater Lett.* 2014;120:94-96. [doi.org/10.1016/j.matlet.2014.01.040](https://doi.org/10.1016/j.matlet.2014.01.040)
20. Termine JD, Peckauskas RA, Posner AS. Calcium phosphate formation in vitro: II. Effects of environment on amorphous-crystalline transformation. *Arch Biochem Biophys.* 1970;140:318-325. [doi.org/10.1016/0003-9861\(70\)90072-X](https://doi.org/10.1016/0003-9861(70)90072-X)
21. Sugiura Y, Munar ML, Ishikawa K. Fabrication of octacalcium phosphate block through a dissolution-precipitation reaction using a calcium sulphate hemihydrate block as a precursor. *J Mater Sci Mater Med.* 2018;29:151-158. [doi: 10.1007/s10856-018-6162-1](https://doi.org/10.1007/s10856-018-6162-1)
22. Fowler BO, Markovic M, Brown WE. Octacalcium phosphate. 3. Infrared and Raman vibrational spectra. *Chem Mater.* 1993;5:1417–1423. [doi:10.1021/cm00034a009](https://doi.org/10.1021/cm00034a009)
23. Mathew M, Brown WE, Schroeder LW, Dickens B. Crystal structure of octacalcium bis hydrogen (phosphate) tetrakis (phosphate) pentahydrate,  $\text{Ca}_8(\text{HPO}_4)_2(\text{PO}_4)_4 \cdot 5\text{H}_2\text{O}$ . *J Crystallogr Spectrosc Res.* 1988;18:235-250. [doi.org/10.1007/BF01194315](https://doi.org/10.1007/BF01194315)
24. Ito N, Kamitakahara M, Murakami S, Watanabe N, Ioku K. Hydrothermal synthesis and characterization of hydroxyapatite from octacalcium phosphate. *J Ceram Soc Jpn.* 2010;118:762-766. [doi.org/10.2109/jcersj2.118.762](https://doi.org/10.2109/jcersj2.118.762)

- 1  
2  
3  
4  
5  
6  
7  
8  
9  
10  
11  
12  
13  
14  
15  
16  
17  
18  
19  
20  
21  
22  
23  
24  
25  
26  
27  
28  
29  
30  
31  
32  
33  
34  
35  
36  
37  
38  
39  
40  
41  
42  
43  
44  
45  
46  
47  
48  
49  
50  
51  
52  
53  
54  
55  
56  
57  
58  
59  
60
25. Ajaxon I, Öhman C, Persson C. Long-Term In Vitro Degradation of a High-Strength Brushite Cement in Water, PBS, and Serum Solution. *BioMed Research Int*, 2015:Article ID 575079. [doi.org/10.1155/2015/575079](https://doi.org/10.1155/2015/575079)
  26. Grover LM, Knowles JC, Fleming GJP, Barralet JE. In-vitro ageing of a brushite calcium phosphate cement. *Biomaterials*. 2003;24:4133-4141. [doi.org/10.1016/S0142-9612\(03\)00293-X](https://doi.org/10.1016/S0142-9612(03)00293-X)
  27. Tung MS, Eidelman N, Sieck B, Brown WE. Octacalcium Phosphate Solubility Product from 4 to 37°C. *J Res Natl Bur Stand*. 1988;93:613-624. [doi.org/10.6028/jres.093.153](https://doi.org/10.6028/jres.093.153)
  28. Ban S, Jinde T, Hasegawa J. Phase Transformation of Octacalcium Phosphate in vivo and in vitro. *Dent Mater J*. 1992;11:130-140. [doi.org/10.4012/dmj.11.130](https://doi.org/10.4012/dmj.11.130)
  29. Yokoi T, Kim IY, Ohtsuki C. Mineralization of calcium phosphate on octacalcium phosphate in a solution mimicking in vivo conditions. *Phosphorus Res Bull*. 2012;26:71-76. [doi.org/10.3363/prb.26.71](https://doi.org/10.3363/prb.26.71)
  30. Liu X, Leng Y. Theoretical analysis of calcium phosphate precipitation in simulated body fluid. *Biomaterials* 2005;26:1097-1108. [doi.org/10.1016/j.biomaterials.2004.05.034](https://doi.org/10.1016/j.biomaterials.2004.05.034)

## Figure Captions

**Figure 1:** SEM images of the prepared spheres (a), (b), and (c) before and (d), (e), and (f) after immersion in acetate buffer for 6 h, at different magnification.

**Figure 2:** SEM images of a whole sphere and pit after immersion in acetate buffer for 6 h. (b) and (c) correspond to the areas indicated in (a).

**Figure 3:** Powder XRD patterns of the spheres after immersion in acetate buffer for various time periods.

**Figure 4:** FT-IR spectra of the spheres after immersion in acetate buffer for 6 h.

**Figure 5:** TEM image (a) and electron diffraction pattern (b) of the spheres after immersion in acetate buffer for 6 h. (b) is with the [110] plane axis of the circled region in (a).

**Figure 6:** *In vitro* degradation of spheres treated with acetate buffer for 6 h in physiological saline (pH 5.4) and phosphate buffered saline (pH 7.4) solutions at 37°C for various time periods (n=4).

**Figure 7:** SEM images of spheres treated with acetate buffer for 6 h in physiological saline (pH 5.4) and phosphate buffered saline (pH 7.4) solutions at 37°C for various time periods.

**Figure 8:** Histograms of the particle size distribution of spheres treated with acetate buffer for 6 h before and after immersion in physiological saline (pH 5.4) and phosphate buffered saline (pH 7.4) solutions at 37°C for 21 days.

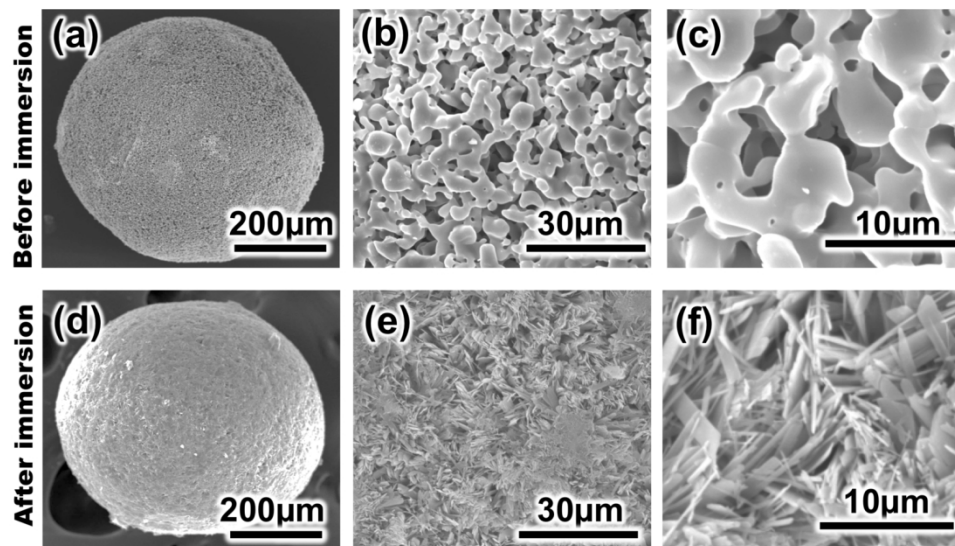


Fig. 1

148x86mm (300 x 300 DPI)

1  
2  
3  
4  
5  
6  
7  
8  
9  
10  
11  
12  
13  
14  
15  
16  
17  
18  
19  
20  
21  
22  
23  
24  
25  
26  
27  
28  
29  
30  
31  
32  
33  
34  
35  
36  
37  
38  
39  
40  
41  
42  
43  
44  
45  
46  
47  
48  
49  
50  
51  
52  
53  
54  
55  
56  
57  
58  
59  
60

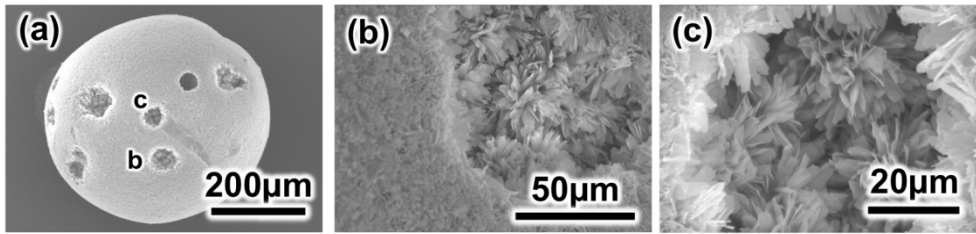


Fig. 2

147x37mm (300 x 300 DPI)

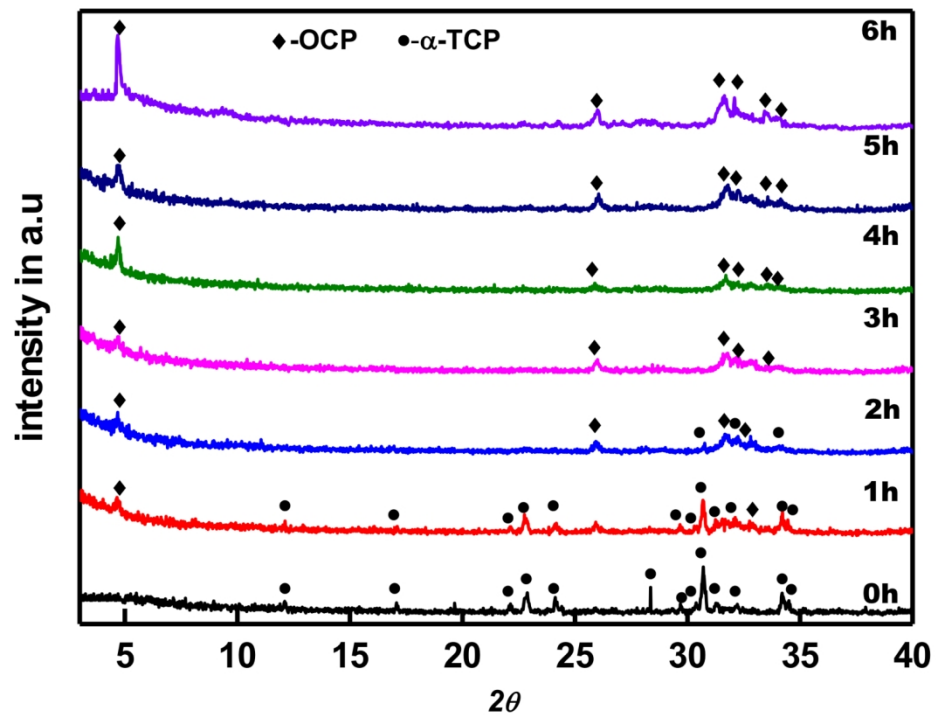


Fig. 3

150x113mm (300 x 300 DPI)

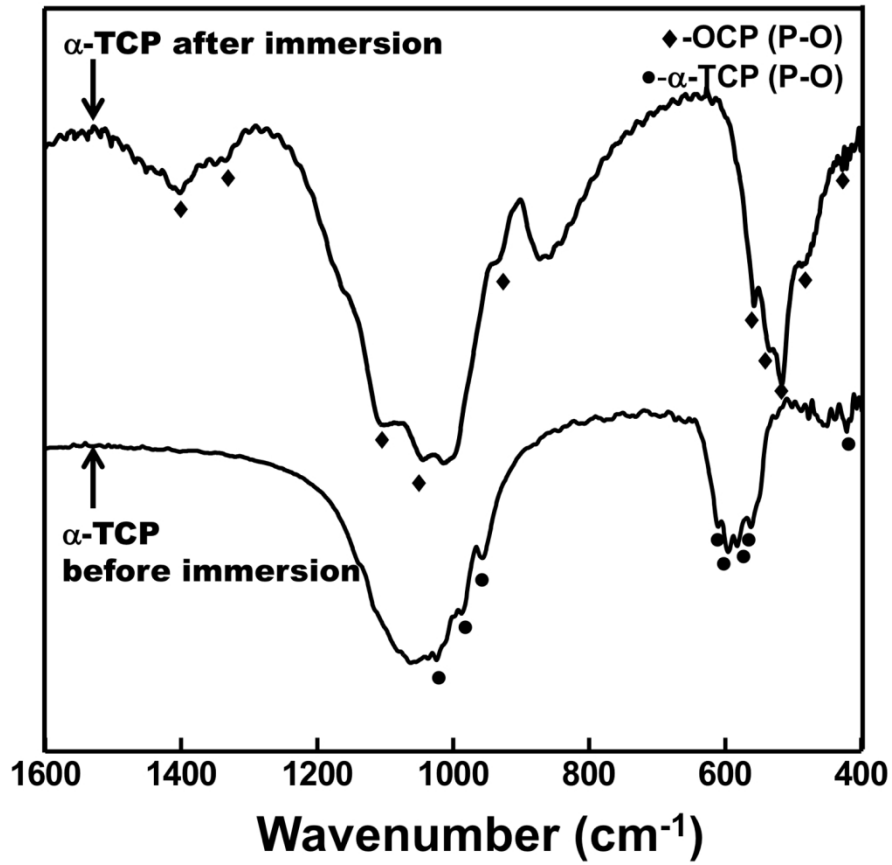


Fig. 4

150x130mm (300 x 300 DPI)

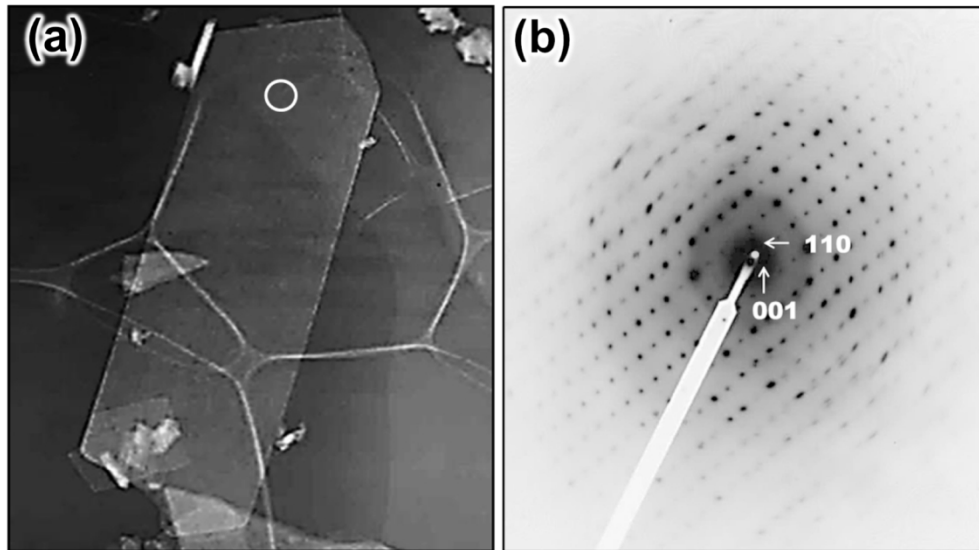


Fig.5

150x83mm (300 x 300 DPI)

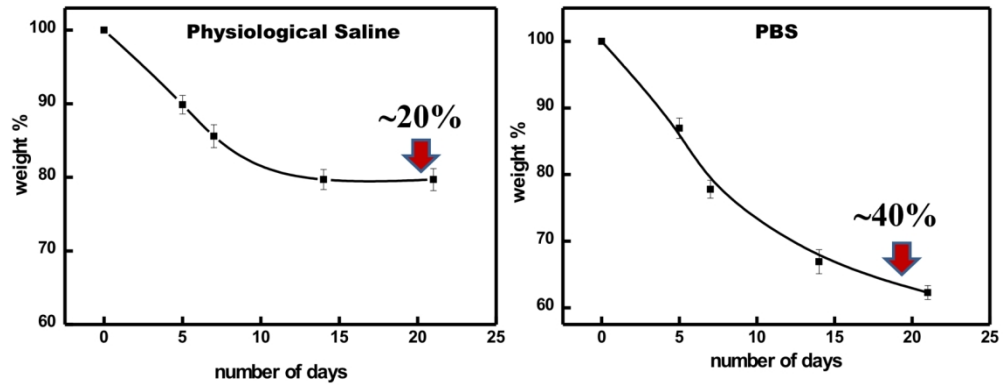


Fig.6

150x62mm (300 x 300 DPI)

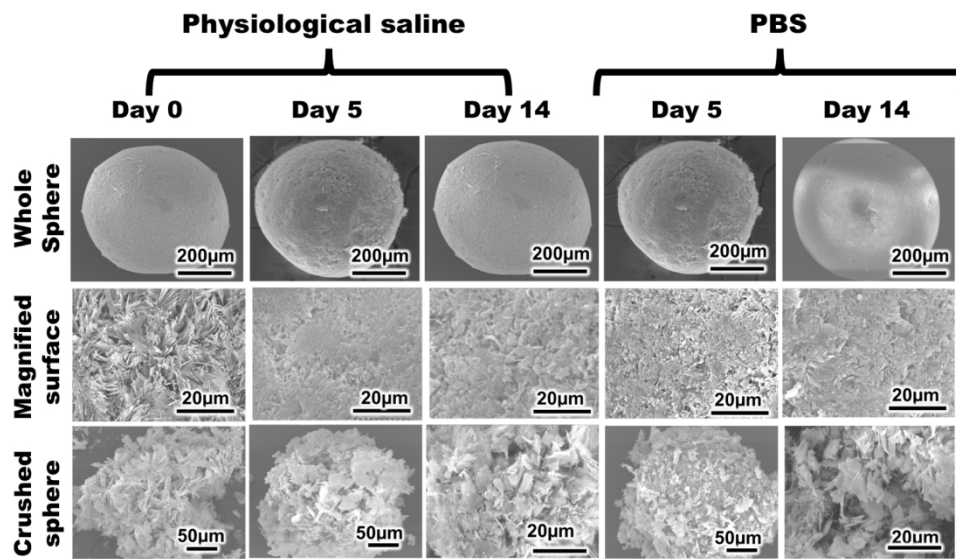


Fig.7

150x89mm (300 x 300 DPI)

1  
2  
3  
4  
5  
6  
7  
8  
9  
10  
11  
12  
13  
14  
15  
16  
17  
18  
19  
20  
21  
22  
23  
24  
25  
26  
27  
28  
29  
30  
31  
32  
33  
34  
35  
36  
37  
38  
39  
40  
41  
42  
43  
44  
45  
46  
47  
48  
49  
50  
51  
52  
53  
54  
55  
56  
57  
58  
59  
60

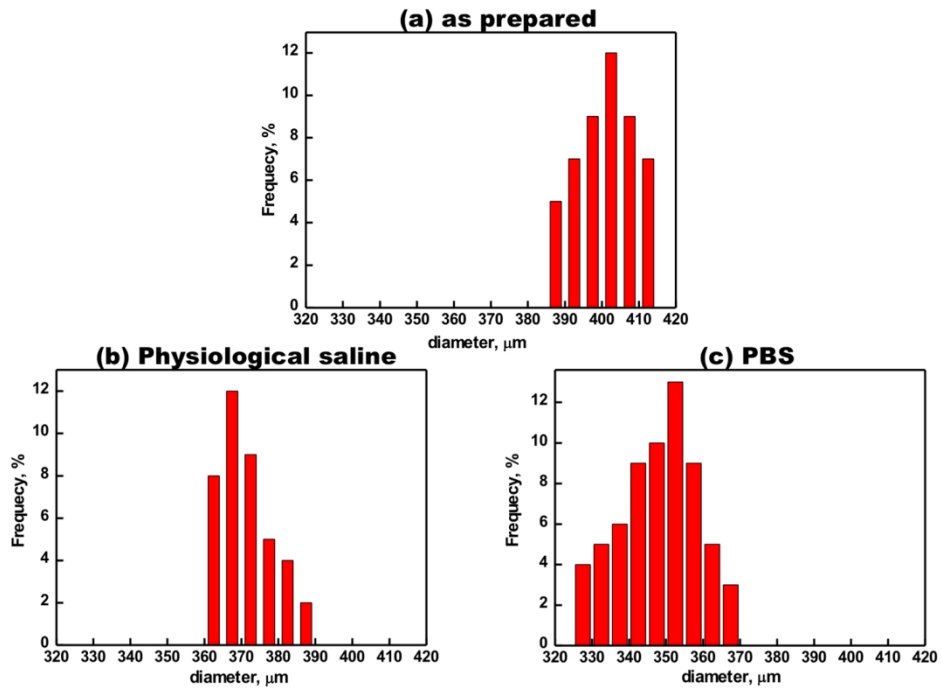


Fig.8

150x108mm (300 x 300 DPI)